

UNIVERSITY OF SOUTHAMPTON
FACULTY OF SOCIAL AND HUMAN SCIENCES
School of Mathematics

Mathematical Modelling of Lithium Ion Batteries

by

Rahifa Ranom

Thesis for the degree of Doctor of Philosophy

October 2014

UNIVERSITY OF SOUTHAMPTON

ABSTRACT

FACULTY OF SOCIAL AND HUMAN SCIENCES

School of Mathematics

Doctor of Philosophy

MATHEMATICAL MODELLING OF LITHIUM ION BATTERIES

by Rahifa Ranom

In this study, we discuss a lithium battery model based on dilute electrolyte theory and fast diffusion of lithium in the electrode particle and calculate some novel solutions to the model. We then discuss moderately concentrated electrolyte theory and outline how homogenisation techniques can be applied to this theory, in combination with a microscale model for lithium transport in the electrode particles in order to derive a Newman type model of the battery [59]. We formulate a numerical method, based on the method of lines in order to solve this model, and apply it to the cases of a half cell graphite anode and a half cell LiFePO_4 cathode. In both scenarios, the results show very good agreement to experimental discharge curves.

Contents

DECLARATION OF AUTHORSHIP	xv
List of Publications	xvii
Acknowledgements	xix
1 Introduction	1
1.1 Lithium batteries as energy storage solution	1
1.2 Battery materials for Lithium ion batteries	3
1.2.1 Desirable electrode and electrolyte properties	3
1.2.2 The cathode material	4
1.2.3 The anode material	4
1.2.4 The electrolyte	5
1.3 Charge-transfer reaction	5
1.4 Battery Terminology	6
1.5 The half-cell	7
1.6 Battery modelling	9
1.6.1 Statement of originality	10
2 Dilute electrolyte modelling of battery	13
2.1 Introduction	13
2.2 Derivation of a model for a dilute electrolyte	13
2.2.1 Charge neutrality	14
2.3 Reaction kinetics on the electrode particle surfaces	15
2.4 The electrode particles	17
2.5 Homogenisation of model accounting for microstructure on electrode particle scale	19
2.5.1 The current collectors	21
2.5.2 The separator	21
2.5.3 The initial conditions	21
2.5.4 The relation between current and global reaction rate	22
2.5.5 Summary of the battery model and comparison to other models	22
2.6 Numerical and analytical solutions for the full cell model	23
Equilibrium solution	24
2.6.1 Nondimensionalization	24
2.6.1.1 Size of dimensionless parameters	26
2.6.2 The Tafel equation approximation for $\Omega_a \ll 1$ and $\Omega_c \ll 1$	27
2.6.3 The quasi steady approximations for $\Gamma \ll 1$	27

2.6.4	Solution for flat discharge curves	28
	Solution before the particles are fully discharged.	29
	Numerical procedure	30
2.6.5	Results and Discussion	30
2.7	The half cell cathode model	33
2.7.1	Quasi-steady state limit $\Gamma \rightarrow 0$	35
2.7.2	Flat discharge curve approximation for LiFePO_4 cathode	36
2.7.3	Analytic solutions	37
	2.7.3.1 Before the development of a free boundary	37
	Numerical solution procedure	38
	2.7.3.2 After development of free boundary	38
	Numerical solution procedure	39
	2.7.3.3 Results and discussion	40
2.8	Summary	41
3	Modelling moderately concentrated electrolytes	45
3.1	Introduction	45
3.2	Stefan-Maxwell equations	46
	3.2.1 Chemical potential ($\bar{\mu}$) and electrochemical potential (μ) of the electrolyte at constant pressure and temperature	46
	Chemical potential	46
	Electrochemical potential	47
3.3	The Stefan Maxwell equations for the binary 1:1 electrolyte	47
	Averaged approximation to Poisson's equation	48
	Non-dimensionalising Poisson's equation	49
	Charge neutrality	50
	Equations for the current density \mathbf{j}	50
	Derivation of the ion velocities in terms of the electrolyte chemical potential μ_e and \mathbf{j}	52
	Diffusion equation for the electrolyte concentration	53
	3.3.1 Summary of model for moderately concentrated electrolyte	53
	3.3.2 An ideal solution	54
	3.3.3 How might we deal with the electric potential	54
	3.3.4 The potential measured with respect to Lithium electrode	55
	Remarks	56
3.4	Thermodynamic fitting to data	56
3.5	Summary	58
4	Review of homogenisation technique for moderately concentrated elec- trolyte model	59
4.1	Introduction	59
4.2	The cell scale electrolyte equations by homogenisation technique	60
	Boundary conditions on the surface of the electrode particles	60
	General set of microscale electrolyte equations.	61
	The asymptotic expansions.	62
	The solution to the moderately concentrated electrolyte model.	64

4.3	Butler-Volmer reaction equations	64
4.3.1	The general version of Butler-Volmer equations for insertion material	64
4.3.2	The Butler-Volmer equations of electrode materials for lithium battery	67
	LiC ₆ anode material	67
	LiFePO ₄ and LiCoO ₂ cathode materials	67
4.4	Summary of the resulting model	68
4.4.1	Boundary conditions for the full cell battery	69
4.5	Summary	70
5	Models for electrode particles	71
5.1	Introduction	71
5.2	Two phase Lithium insertion/extraction	71
5.2.1	"Shrinking-core" model	73
	Nondimensionalisation	74
5.2.1.1	Solution Procedure	76
5.2.1.2	Asymptotic solution of shrinking core diffusion	77
	Summary.	78
5.2.2	Phase-field model	79
5.3	More than two phases	80
5.4	Diffusion equation in the spherical coordinate	81
	Current density in the electrode	81
5.5	Summary	82
6	Numerical Procedure	83
6.1	Introduction	83
6.2	Method of Lines	85
6.3	Development of sparse matrix for the system	86
6.3.1	The development of the solution vector \mathbf{u}	87
6.3.2	The development of matrices for electrolyte concentration, c	88
	Summary	89
6.3.3	The development of matrices for electrolyte potential, $\hat{\phi}$	89
6.3.4	The development of matrices for the electrode potential, $\hat{\phi}_s$	90
6.3.5	The development of matrices for concentration in the electrode particles, c_s	91
6.3.6	The development of \mathbf{A} , \mathbf{M} and \mathbf{f}	93
6.4	ode15s	93
	Convergence	94
6.5	Summary	96
7	The Half cell Anode	97
7.1	Introduction	97
7.2	The half cell anode model	97
7.3	Nondimensionalisation	99
	Remarks.	99
	Discussion of dimensionless parameters	101
7.4	Model - experimental comparisons for the natural graphite electrode	102
7.4.1	Results and Discussions	104

7.4.1.1	An approximation solution	107
	Summary	108
7.4.1.2	Concentration-dependent of diffusion coefficient	108
7.5	Summary	112
8	Half cell cathode	115
8.1	Introduction	115
8.2	Transport data and parameter values used in the simulation	116
8.2.1	Nondimensionalisation	118
	Parameter Values	119
	Numerical Procedure	121
8.3	Model-experimental comparison	121
8.4	The effects of parameter variations on the discharge of a nanostructured half-cell cathode	123
8.5	Summary	136
9	Conclusions and Future Works	137
9.1	Conclusions	137
9.2	Future works	139
	The effect of different sizes of particles	139
	The effect of changes in particle shape and packing upon cell performance	139

List of Figures

1.1	A schematic diagram of the Lithium Ion Battery during discharge [59]. The current flowing out of the positive electrode drives the extraction of lithium ion from negative electrode (anode) particles to the electrolyte across the porous separator (by diffusion and advection) into the positive electrode (cathode) and insert into the positive electrode (cathode). The charge of electrons are moving from the negative electrode particles to the negative electrode current collector and from the positive electrode current collector to the positive electrode particles.	2
1.2	Structure of the electric double layer near a solid electrolyte interface when external electric field is applied. The electric drops linearly from the electrode potential ϕ_s to the electrolyte potential ϕ in a thin layer. . .	6
1.3	Schematic diagram for typical half cell anode. The cathode material is a lithium-foil which is reacting as reference electrode. During discharge, the Lithium ions are conducted through the electrolyte solution to the lithium electrode. Here $x^* = 0$ is the anode current collector and $x^* = L$ is the separator.	8
1.4	A schematic diagram for a typical half-cell cathode. The anode material is a lithium-foil. Here $x^* = 0$ is the separator and $x^* = L$ is at cathode current collector	8
2.1	Reaction rate on the solid electrolyte interface in anode and cathode. . . .	15
2.2	Different types of open circuit potential i.e. $U_{eqc}^*(y)$ curves for different cathode materials with respect to the insertion chemistry of the materials, y (normalized capacity).	17
2.3	Different types of open circuit potential i.e $U_{cqa}^*(x)$ curves for different anode materials with respect to the insertion chemistry of the materials, x (normalized capacity).	18
2.4	Schematic representation of the mathematical domains in particle scale. . .	20
2.5	The solution of dimensionless electrolyte potential, $\tilde{\phi}(x)$ from (symbols) analytical expression (2.91) compared to (line) numerical simulation using MATLAB 'bvp4c' at discharge current $\bar{I} = 1.32$	31
2.6	Graph of dimensionless electrolyte concentration $c(x)$ at different discharge currents $\bar{I} = 1.0, 1.2, 1.4, 1.7$ as a function of position. This analytical solutions are obtained by equation (2.91).	32
2.7	Graph of dimensionless electrolyte potential $\tilde{\phi}(x)$ at different discharge currents $\bar{I} = 1.0, 1.2, 1.4, 1.7$ as a function of position. This figure is obtained by relation to the electrolyte concentration as stated in (2.77). . .	32

2.8	Dimensionless intercalated Lithium concentration distribution in the particle for anode ($0 < x < 1$) and cathode ($1 < x < 2$), c_{sa} and c_{sc} respectively (by solving (2.88)-(2.90) numerically) for discharge current (a) $\bar{I} = 1$ and (b) $\bar{I} = 1.5$. Here $0 < x < 1$ is the anode and $1 < x < 2$ is the cathode. The profiles are measured at $t^* = 100s, 200s, 300s, 400s, \dots$	34
2.9	The free boundary problem; (a) $x < s(t)$ - Cathode particles are full with Lithium ($c_{sc} = 1$) and (b) $x > s(t)$ - Cathode particles are partially filled ($c_{sc} < 1$)	36
2.10	Dimensionless concentration profiles of the model before the free boundary develops by (symbol) analytical solution (2.119) and (solid line) numerical simulation for $\bar{I} = 1$.	40
2.11	Lithium ion concentration distribution in the solid particles by equation (2.122) at $\bar{I} = 1$. The profiles are measured at $t = 0.05, 0.1, 0.15, 0.2, \dots$. At certain time ($t = \hat{t}$), the concentration in the solid reaches maximum ($c_{sc} = 1$) in region near separator and at later time ($t > \hat{t}$), free boundary develops. Here $\hat{t} = 0.55$	41
2.12	(a) Upper figure: the concentration of lithium in solid particles that reaches the maximum capacity at $x = s(t)$. The solubility rate of lithium no longer at the same rate at this point forward because of the concentration profiles of electrolyte. (b) Lower figure: The concentration profiles across the cell in comparison to the time before ($t < \hat{t}$) (by equation (2.119)) and after ($t > \hat{t}$) (by equation (2.132)) formation of free boundary. The profiles are discharged at $\bar{I} = 0.5$. The arrow shows the direction of increasing time and $\hat{t} = 0.64$.	43
2.13	The concentration of Lithium in solid particles and Lithium ions electrolyte at $\bar{I} = 1$ discharge rate. The arrow shows the direction of time increases ($t = 0.55, 0.6, 0.65, \dots$) and $\hat{t} = 0.55$.	44
3.1	Structure of the electric double layer near a solid/electrolyte interface. When external electric field is applied, bulk motion of an electrolyte caused by Coulombic forces acting on ions in the electric double layer. The electric double layer, composed of a Stern layer(layer 1), Debye layer(layer 2) and bulk solution(layer 3). The bottom graph shows the difference of potential energy in each layer before the mobile ions extending into the bulk solution.	49
3.2	Diffusion coefficient as a function of concentration; line represents the fit to (3.71) and circles are the experimental data from Riemers [90].	57
3.3	Concentration-dependent of electrolyte conductivity; line represents the fit to (3.72) and circles are the experimental data from Riemers [90].	57
4.1	Illustration of the microstructured boundary	63
5.1	Illustration of the shrinking-core model with the side by side of the two phases and the movement of the phase boundary. The processes during discharge are illustrated and the pictures below showing concentration of Lithium as a function of r for different times. The dark region represents the Lithium-rich region and the bright region represents the Lithium-poor region.	73

- 7.8 The comparison of non linear diffusion coefficient-experimental data for the graphite half cell discharge curves at different currents. The curves are obtained by analytic approximation solution (7.34) where the diffusion equation in the solid (see (7.23)-(7.24)) is solved numerically. The nonlinear diffusion coefficient (the fitting to the data from Zhang *et al.* [102]) is given by equation (7.36). Solid lines represent the analytic solutions and symbols represent experimental data at various discharge currents. The dashed curve represents the equilibrium potential curve. 112
- 7.9 The dimensionless concentration of Lithium within the electrode particle at $3C$ discharge rate where $D_s(c_s)$ is calculated using data from Zhang *et al.* [102] (see formula (7.36)). The profiles are measured at $t^* = 30s, 60s, 90s, 120s, 150s$ 113
- 8.1 The equilibrium potential of the LiFePO_4 electrode as a function of c_s (the state of discharge, $c_s = c_s^*/c_{max}$) (see equation (8.27)). 120
- 8.2 The comparison of model with the experimental data for the LiFePO_4 half cell discharge curves at different currents. Solid lines represent the analytic solutions and symbols represent experimental data at various discharge currents. 123
- 8.3 The concentration of solution in the electrolyte across the electrode at (a) $0.8C$ and (b) $3.2C$ discharge rate. The profiles are measured at (a) $t^* = 393s, 785s, 1178s, 1571s, 1963s$ and (b) $t^* = 162s, 325s, 487s, 585s, 650s$ 124
- 8.4 The concentration of Lithium in the solid at the electrode particle surfaces as a function of position in the electrode at (a) $0.8C$ and (b) $3.2C$ discharge rate. The profiles are measured at (a) $t^* = 393s, 785s, 1178s, 1571s, 1963s$ and (b) $t^* = 162s, 325s, 487s, 585s, 650s$ 125
- 8.5 The reaction rate (per unit surface area) at the particle electrolyte interface as a function of position in the electrode for discharge at $3.2C$. The profiles are measured at $t^* = 162s, 325s, 487s, 585s, 650s$ 126
- 8.6 The dimensionless concentration in the electrode particle as a function of radius at different positions in the electrode for discharge at $3.2C$. The profiles are measured at $t^* = 162s, 325s, 487s, 585s, 650s$ 126
- 8.7 The concentration of solution in the electrolyte across the electrode at $8C$ discharge rate. The profiles are measured at $t^* = 33s, 48s, 58s, 62s, 65s$ 127
- 8.8 The concentration of Lithium in the solid at the electrode particle surfaces as a function of position in the electrode at $8C$ discharge rate. The profiles are measured at $t^* = 33s, 48s, 58s, 62s, 65s$ 127
- 8.9 The voltage curves for different conductivity ratios in the solid (σ_s) and electrolyte (κ_{max}) phases. The cell is discharged at $1.6C$ 128
- 8.10 The dimensionless solid concentration profiles at the electrode particle surfaces as a function of position in the electrode for different conductivity ratios in the solid (σ_s) and electrolyte (κ_{max}) phases. The cell is discharged at $1.6C$ 129
- 8.11 The electrolyte concentration profiles across the electrode for different conductivity ratios in the solid (σ_s) and electrolyte (κ_{max}) phases. The cell is discharged at $1.6C$ 130
- 8.12 The dimensionless solid concentration profiles in the electrode particles as a function of radius at different positions when the cell is discharged for the 3 different cases. The cell is discharged at $1.6C$ 132

DECLARATION OF AUTHORSHIP

I, **Rahifa Ranom**, declare that the thesis entitled **Mathematical Modelling of Lithium Ion Batteries** and the work presented in the thesis are both my own, and have been generated by me as the result of my own research. I confirm that:

- this work was done wholly or mainly while in candidature for a research degree at this University;
- any part if this thesis has previously been submitted for a degree or any other qualification at this University or any other institution, this has been clearly stated;
- where I have consulted the published work of others, this is always clearly attributed;
- where I have quoted from the work of others, the source is always given. With the exception of such quotations this thesis entirely my own work;
- I have acknowledged all main sources of help;
- where the thesis is based on work done by myself jointly with others, I have made clear exactly what was done by others and what I have contributed myself;
- parts of this work have been published.

Signed:

Date: *31st October 2014*

List of Publications

1. Ranom R., Richardson G., Please C., (2011). **Steady state solution during discharge in lithium ion batteries with Tafel kinetics**, International Conference of Chemical Engineering and Industrial Biotechnology (ICCEIB), November 28 - December 1, 2012, Pahang, Malaysia.
2. Ranom R., Richardson G., Please C.P., (2012). **Discharge of half cell cathode of lithium ion battery**. British Applied Mathematics Colloquium (BAMC), April 6 - 9, 2012, London, UK.
3. Adesokan B., Ayass W.A., Lim S., Peace A, & Rahifa R., (2013), **Assessing molecular properties for oral drug delivery.**, 5th UK Graduate Modelling Camp, April 9-12 2013, Oxford, UK.
4. Rahifa R., Foster J.M., Richardson G., (2014), **Mathematical modelling of half-cell Lithium ion battery in moderately dilute solution.**, International Meeting of Lithium Batteries, June 10-14 2014. Lake Como, Italy.

Acknowledgements

Thanks to Almighty Allah S.W.T. for graciously bestowing me the perseverance to undertake this research. Special thanks are due to: University of Southampton for the opportunity to carry out research; Universiti Teknikal Malaysia Melaka (UTeM) for the financial support and Kementerian Pengajian Tinggi (KPT). Warmest thanks and a deepest appreciation to the following people: My parents, Ranom and Hamidah, for a lifetime of love and support; My lovely husband, Ahmad Fuad, for an eternity love and full support; My academic father, Dr. Giles Richardson, for all his help and expert advice, for the encouragement and inspiration; Dr. Jamie Foster, for his numerical expertise; My daughter and son, Arissa Humaira and Isyhadh Umayr, for make my life full of happiness and laughters; My family and friends, for all their support and for sharing me so often with my problems.

Chapter 1

Introduction

The demand for more efficient renewable energy resources is rapidly growing as energy and environmental based issues becomes of increasing concern. Lithium ion batteries are currently the state of art of rechargeable electrochemical storage devices. These batteries provide high volumetric energy densities, high cyclability and are highly flexible as regards to design, size and application. They are used in many applications in portable electronics such as mobile phones, laptops and power tools; and are being considered for use in electric vehicles. Lithium ion batteries have thus gained much attention from researchers worldwide. Moreover, the development of lithium batteries has become a key focus for researchers in automotive companies who are investigating their use in hybrid electric vehicles (HEV), plugin hybrid vehicles (PHEV), and purely electric vehicles (EV); the markets for all of which are expected to grow substantially in the future years.

1.1 Lithium batteries as energy storage solution

The lithium ion battery is one of the most successful electrochemical batteries and billion of these cells are produced every year. They provide rechargeable energy storage at high energy density, with no memory effect, and slow loss of charge when not in use [11]. They are of growing interest to the automotive industry, amongst others. Thus, there is a big drive to increase their efficiency, storage performance and the speed at which they can be charged and recharged. Many approaches have been taken to simulate the operation of such devices in order to better understand their behaviour.

The Lithium ion cell consists of four parts, namely (I) the anode which is comprised of negative electrode particles, (II) the cathode which is comprised of positive electrode particles, (III) the separator that lies between the electrodes (this is a porous insulator that prevents direct electrical contact between the electrodes while allowing passage of

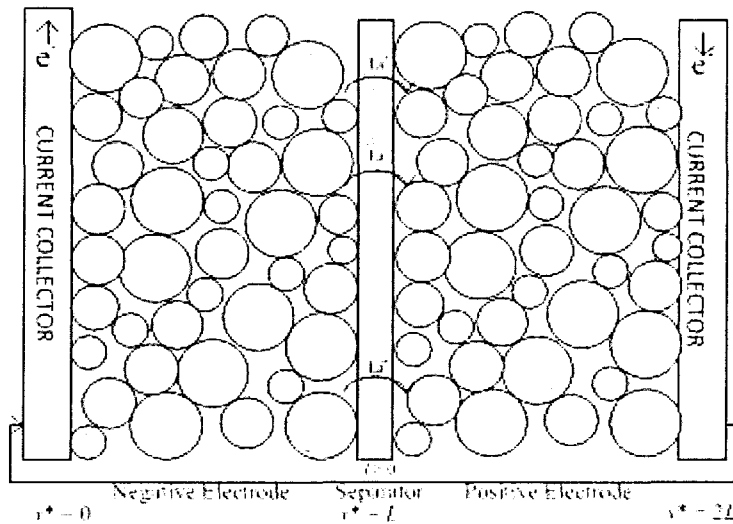


Figure 1.1: A schematic diagram of the Lithium Ion Battery during discharge [59]. The current flowing out of the positive electrode drives the extraction of lithium ion from negative electrode (anode) particles to the electrolyte across the porous separator (by diffusion and advection) into the positive electrode (cathode) and insert into the positive electrode (cathode). The charge of electrons are moving from the negative electrode particles to the negative electrode current collector and from the positive electrode current collector to the positive electrode particles.

the electrolyte) and (IV) the Lithium ion electrolyte which transports ions (and thus charge) between the anode and cathode. A schematic diagram of such a cell (during discharge) is shown in Figure 1.1. At the outer boundaries of electrodes there are current collectors (charge collectors) that connect to an external circuit.

During discharge, Lithium diffuses through the negative electrode (anode) particles to the solid-electrolyte interface where it undergoes a charge transfer reaction (refer Figure 1.1) in which a Lithium ion (Li^+) is released into the electrolyte and an electron (e^-) is released into the electrode particle (de-intercalation). The Lithium ion advects, and diffuses, through the electrolyte solution to the positive electrode (cathode). A similar reaction occurs on the surface of a positive electrode (cathode) particle in which the Lithium ion is absorbed into the electrode particle (by a process known as intercalation) and takes up an electron from the electrode as it does so. The negative ions (N^-), on the other hand, remain in the electrolyte throughout. Thus the Lithium ions (Li^+) carry all the charge through the electrolyte (and separator diaphragm) from the anode to cathode. Typically, the reaction rate on an electrode particle surface depends upon the lithium concentration on the electrode surface, the lithium ion concentration in the adjacent electrolyte, and the potential drop between the electrode and electrolyte [36]. When the cell is charging, the process is reversed: an external electrical power source (the charging circuit) applies a higher voltage than that produced by the battery, forcing

current to pass in the reverse direction. The Lithium ions then migrate from the cathode to the anode, where they become embedded in the electrode material (intercalation).

The anode and cathode materials are selected so that the anode preferentially gives up electrons (and thus also lithium ions), and the cathode preferentially accepts electrons (and thus lithium ions). The tendency of a material to give up or accept electrons is determined by its standard electrode potential. The difference in the standard electrode potential of the anode and the cathode gives the voltage of the cell at equilibrium (the potential difference between the current collectors). The equilibrium potential is the difference between the electrical potential of the two current collectors when no external electric current flows between them. It is a function of the electrode materials used. In the following sections, an overview of battery materials for Lithium ion rechargeable batteries is provided.

1.2 Battery materials for Lithium ion batteries

Typically, both electrodes (anode and cathode) in a lithium ion battery are intercalation compounds, that is, they have a lattice structure in which small atoms, such as lithium, can be inserted and extracted. In contrast, the electrolyte allows the flow of electrical charge (in the form of lithium ions) between the anode and cathode. This section reviews battery materials for anodes, cathodes and electrolytes.

1.2.1 Desirable electrode and electrolyte properties

In designing a battery, the properties of electrode materials and electrolytes are important in order to achieve a successful cell once they are assembled. They should, for example be chosen so that the cell is stable and safe to minimize the risk of short circuits. The key requirements for a successful electrolyte are high conductivity (high mobility of Lithium ions), stability (at high temperatures and in high voltage application) [82], and safety (low flammability [10]). Electrolyte decomposition and side reactions in lithium ion batteries can create thermal runaway [11]. Thus, the electrolyte selection has to balance between flammability and electrochemical performance.

Good electrode materials should have high lithium diffusivity in the host matrix; high electrical conductivity; stability (not change structure over many charge cycles); high capacity [95]; thermal stability [10], high cyclability and be non toxic and low cost [11]. The two electrode materials also be chosen to give the cell a high voltage. The solid electrolyte interface (SEI layer) is another key factor that influences the performance of battery. The roles of this layer is to eliminate the transfer of negative ions from the electrolyte to the electrodes and to limit the transfer of electrons from the electrodes to the electrolytes [48]. However, the SEI layer must also be a good Lithium ion conductor.

1.2.2 The cathode material

In 1991, the first type of cathode material to go into commercial production, was cobalt oxide (LiCoO_2) [95]. It (de)intercalates lithium ions at around $4V$ and has a theoretical capacity of 140 mAh/g [88]. The other advanced cathode materials include lithium metal oxides (such as LiMn_2O_4), olivines (such as LiFePO_4), and rechargeable lithium oxides [82].

In 1996, Goodenough patented a new kind of lithium ion cathode material which is iron phosphate LiFePO_4 [65]. This material is more powerful and less likely to catching fire, which are important considerations for automotive applications. LiFePO_4 has already found in many industrial applications due to its reasonable voltage of $3.5V$, high theoretical capacity (170 mAh/g) [52], low cost, low toxicity, and high thermal stability [65]. Because of its potential, much research has been directed towards optimizing synthesis routes for LiFePO_4 cathodes. A disadvantage of this material is low conductivity. However carbon coating of the electrode particles increases the conductivity of the electrode [47]. LiFePO_4 is also thermodynamically stable [67], and its has a lattice structure so that the insertion/extraction lithium ions process does not change structure of the host material [95].

Lithium metal oxides contain cobalt and nickel. They show a high stability in the high-voltage range but cobalt has limited availability in natural resources and is toxic [22]. Manganese offers very good rate capabilities but has poor cycling behaviour. Therefore, mixtures of these three materials are often used for a good cathode material.

1.2.3 The anode material

The commercial anode material in lithium ion batteries is graphitic carbon (LiC_6) which can store up to one Li^+ for every six carbon atoms in between its graphene layers. The material is highly conducting and supports high current densities [13]. However, the theoretical capacity (372 mAh/g) is poor in comparison to that of pure lithium ($3,862 \text{ mAh/g}$) [97] and it exhibits moderate charge/discharge rate performance which limits the lifetime of the cell [69]. The parameters used to increase the performance of this anode material are its thickness, and its porosity.

Alloy anodes such as Li-Al (Lithium Aluminium) have high capacities but exhibits substantial volume changes, which results in low cyclability [22]. Reducing the size of this electrode particles to the order of a few nanometres stops phase transitions occurring that typically accompany alloy formation [10] and reduces the size of the volume changes. Lithium titanate operates at a $2.4V$, a voltage for which lithium ions are stable with respect to the electrolyte [11] (which is a requirement in this material because it does not form an SEI layer). A disadvantage of the lithium titanate battery is lower capacity and voltage than the conventional anode material. Silicon has an extremely high

capacity (4,199 *mAh/g*) corresponding to a composition of $\text{Si}_3\text{Li}_{22}$ [22]. However, the large volume changes that occur during the insertion and extraction processes cause severe cracking of the electrode, which in turn leads to very significant capacity fade during cycling [98]. The cyclability of this electrode can be improved by adding Ketjen-black carbon, which gives a chainlike structure that maintains a stable electronic contact between silicon particles [98]. They can also be improved by nanostructuring [10].

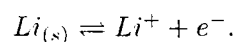
1.2.4 The electrolyte

Liquid electrolytes conduct lithium ions and acting as a carrier between the cathode and the anode. The electrolytes typically used in lithium ion cells are mainly based on an organic solvent based. Examples of electrolyte salts used in applications include lithium hexafluorophosphate (LiPF_6), lithium hexafluoroarsenate monohydrate (LiAsF_6), lithium perchlorate (LiClO_4), lithium tetrafluoroborate (LiBF_4), and lithium triflate (LiCF_3SO_3). LiClO_4 provides a stable charge-discharge efficiency that increases the cycling capacity of the cell [10]. LiBF_4 is less toxic than LiAsF_6 and safer than LiClO_4 but has only moderate ionic conductivity [47]. LiCF_3SO_3 is resistant to oxidation, nontoxic, thermally stable, and insensitive to ambient temperature in contrast to LiPF_6 . However, it has low conductivity in nonaqueous solvents as compared to other salts [47].

Currently, LiPF_6 is the standard electrolyte in commercial batteries. It has qualities such as high conductivity, high solubility in organic solvents, and stability in the solvents mixture and on common electrode materials [22]. The organic solvent that often used in battery electrolyte is a mixture of ethylene carbonate and dimethyl carbonate (1:1 EC:DMC). Ethylene carbonate (EC) has ability to form a good SEI layer on common anode materials and dimethyl carbonate (DMC) has ability to lower the EC melting point [22]. In this study, we chose the most common electrolyte solution, which is LiPF_6 salts dissolved in a mixture of 1:1 EC:DMC. This combination performs well enough in current battery systems.

1.3 Charge-transfer reaction

The reactions in which charges are transferred across a solid electrolyte interface are called charge transfer reactions. Here both electrodes are either oxidized or reduced:



Charge separation occurs when charge transfers across the electrode surface. The excess charge on the electrode surface is counterbalanced by the accumulation of oppositely

charged ions, on the electrolyte phase. The layer across which this charge separation occurs is called the electrical double layer, and is extremely thin (typically of order 1nm) compared with the width of the electrolyte and electrodes. In its simplest form the double layer is described by the Helmholtz model, which describes the double layer as a parallel plate capacitor with a small plate separation (see Figure 1.2). In this model, the potential changes linearly from the electrode potential ϕ_s to the electrolyte potential ϕ in a thin layer. This layer is referred to as the Helmholtz layer.

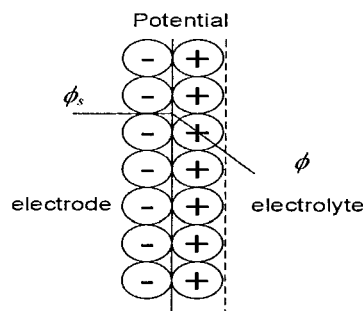


Figure 1.2: Structure of the electric double layer near a solid electrolyte interface when external electric field is applied. The electric drops linearly from the electrode potential ϕ_s to the electrolyte potential ϕ in a thin layer.

The electrical double layer translates into boundary layers in the concentration profiles. Near an electrode that is negatively charged we expect an excess of Li^+ ions and a deficit of N^- ions. These differences are only expected close to the electrode surface, thus it is usual to assume charge neutrality in the bulk of the solution. Further details on charge neutrality will be discussed later. The overpotential, $q\eta$ is defined such that η gives the change in the electrochemical potential of a Li^+ between the electrolyte and the electrode. It takes the form

$$\eta = \phi - \phi_s + U_{eq}$$

where ϕ is the electrolyte potential, ϕ_s is the solid potential and U_{eq} is the equilibrium potential of the electrode material (qU_{eq} is the change in chemical potential of Li^+ ion between the electrode and electrolyte). The equilibrium potential, or open circuit potential, is the difference of electrical potential between the two terminals of a device when there is no electric current flows between them. Usually it is measured at a very low discharge rate.

1.4 Battery Terminology

- **Capacity.** The capacity is a measurement of how many electrons can be extracted from an electrode during each charge or discharge cycle and has unit in

milliamp hours per gram. A symbol Q is used for this parameter. This quantity is often normalized by mass, so that it is unaffected by the size of the battery. The maximum capacity of a cell is determined by the amount of charge when the cell is discharged at a very low rate. Current cathode materials have maximum capacities in the range of $Q_{max} = 100 - 200mAh/g$ and graphitic carbon (the most common anode material) which has a maximum capacity of around $Q_{max} = 300mAh/g$.

- **Specific Power.** Another important parameter for battery operation is how much power can be provided per unit mass. This value, measured in watts per kilogram, is particularly important for high power applications such as acceleration of electric vehicles where a large amount of energy must be provided in a short time. Specific power is heavily influenced by the voltage difference between the anode and cathode and the speed of ion transfer between the electrodes.
- **Cell Voltage.** A key parameter in maximizing the specific power of a battery is the voltage difference between the anode and cathode. This difference is determined by the relative voltages at which the (de)intercalation reactions take place. In this thesis, discharge curves are plotted showing the cell voltage as a function of the state of discharge and at certain specific discharge rates.
- **Discharge rate, C-rate.** The discharge rate is the rate at which current is taken from a cell. It is reported as a C-rate with $1C$ corresponding to a battery being completely charged or discharged in one hour. High rate capability is essential for quick charging batteries and high power applications. For instance, for a battery with a capacity of $100A/hours$, this equates to a discharge current of $100Amps$. A $5C$ rate for this battery would be $500Amps$, and a $C/2$ rate would be $50Amps$.
- **State of charge / discharge.** The state of charge (SOC) is defined as the capacity still available in the cell. It is normally expressed as a ratio of the rated capacity to the maximum capacity and a 0 SOC battery is fully discharged while a 1 SOC battery is fully charged battery. The state of discharge (SOD) is defined as the ratio of battery capacity that has been discharged to the maximum capacity. State of charge/discharge can be calculated as the current multiplied by the time and divided by the maximum capacity of the cell (It/Q_{max}).

1.5 The half-cell

In order to test a particular electrode in the lab it is usual to perform experiments on a half-cell. This consists of a single electrode (working electrode either anode or cathode) and a pure Lithium electrode (reference electrode) as the other electrode (see Figures 1.3 and 1.4). Since the electrochemical potential of lithium in a lithium electrode does not change as it charges / discharges, it also acts as a reference electrode. Indeed in

charged ions, on the electrolyte phase. The layer across which this charge separation occurs is called the electrical double layer, and is extremely thin (typically of order 1nm) compared with the width of the electrolyte and electrodes. In its simplest form the double layer is described by the Helmholtz model, which describes the double layer as a parallel plate capacitor with a small plate separation (see Figure 1.2). In this model, the potential changes linearly from the electrode potential ϕ_s to the electrolyte potential ϕ in a thin layer. This layer is referred to as the Helmholtz layer.

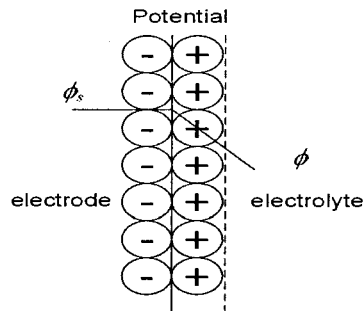


Figure 1.2: Structure of the electric double layer near a solid electrolyte interface when external electric field is applied. The electric drops linearly from the electrode potential ϕ_s to the electrolyte potential ϕ in a thin layer.

The electrical double layer translates into boundary layers in the concentration profiles. Near an electrode that is negatively charged we expect an excess of Li^+ ions and a deficit of N^- ions. These differences are only expected close to the electrode surface, thus it is usual to assume charge neutrality in the bulk of the solution. Further details on charge neutrality will be discussed later. The overpotential, $q\eta$ is defined such that η gives the change in the electrochemical potential of a Li^+ between the electrolyte and the electrode. It takes the form

$$\eta = \phi - \phi_s + U_{eq}$$

where ϕ is the electrolyte potential, ϕ_s is the solid potential and U_{eq} is the equilibrium potential of the electrode material (qU_{eq} is the change in chemical potential of Li^+ ion between the electrode and electrolyte). The equilibrium potential, or open circuit potential, is the difference of electrical potential between the two terminals of a device when there is no electric current flows between them. Usually it is measured at a very low discharge rate.

1.4 Battery Terminology

- **Capacity.** The capacity is a measurement of how many electrons can be extracted from an electrode during each charge or discharge cycle and has unit in

applications it is usual to define potential with respect to a lithium electrode such that its potential is defined to be zero. The voltage drop across the half cell is then determined by the potential of the current collector. This motivated Newman to formulate his models [60] in terms of a lithium reference potential rather than the real potential. Theoretical treatment of half-cells include works by Newman et. al. [84] and Farrell et.al. [23]. Fundamental research on electrode material is usually conducted in half-cell systems. Figure 1.3 shows a schematic diagram of a half-cell anode and Figure 1.4 that for a half-cell cathode.

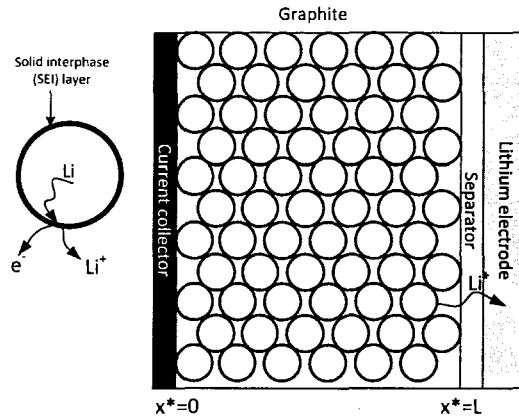


Figure 1.3: Schematic diagram for typical half cell anode. The cathode material is a lithium-foil which is reacting as reference electrode. During discharge, the Lithium ions are conducted through the electrolyte solution to the lithium electrode. Here $x^* = 0$ is the anode current collector and $x^* = L$ is the separator.

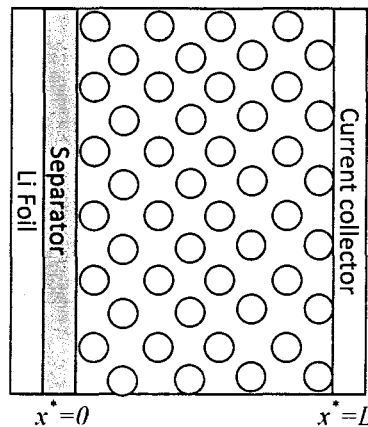


Figure 1.4: A schematic diagram for a typical half-cell cathode. The anode material is a lithium-foil. Here $x^* = 0$ is the separator and $x^* = L$ is at cathode current collector

takes place on the surface anode and hence increased the resistances on the surface of anode particle. Safari *et al.* [77] simulated the ageing phenomena in a commercial graphite/LiFePO₄ cell.

The effects of interionic drag in non-dilute solution has been incorporated into Newman framework [60] but requires the model to be calibrated again experimental electrolyte data. An example of such data is found in the work of Riemers *et. al* [90] which measures conductivity, diffusivity and transference number as function of ions concentration in the electrolyte LiPF₆ in 1:1 EC:DMC. Fuller, Doyle and Newman [28, 36] incorporated the effects of the chemical activity in the electrolyte into their modelling framework.

Recent work has shown that performance of Lithium ion battery can be improved through emphasis on engineering the microstructural architecture of the electrodes see [41, 83, 39]. Typically the effects of the microstructure in macroscopic models, such as Newman's [58], are represented by a few phenomenological parameters which can be crudely related to the properties of the microstructure. A more systematic approach, that is capable of relating the geometry of the microstructure coefficients in the macroscopic model, has been developed by Richardson *et.al* [74] in the case of dilute electrolytes. Here we shall extend this method to a moderately concentrated electrolyte.

Solutions to a battery model based on a dilute electrolyte model in which Lithium diffusion in the electrode particles is extremely fast are discussed in Chapter 2. In Chapter 3 we discuss an electrolyte model of a moderately concentrated electrolyte and fit the model to real electrolyte diffusion, conductivity and transference number data. In Chapter 4, we discuss the application of homogenisation techniques to a model based on the moderately concentrated electrolyte model discussed in Chapter 3. In Chapter 5, we discuss Lithium transport in electrode particles (in particular the LiFePO₄ and the LiC₆ electrode materials), this is crucial for understanding intercalation. In Chapter 6, we discuss the numerical method that we use to solve the homogenised model presented in Chapter 4. Solutions to the model are compared against experimental data for half-cell Li_xC₆ (graphite) anodes (Chapter 7) and half-cell LiFePO₄ cathodes (Chapter 8). Finally, we draw our conclusions in Chapter 9.

1.6.1 Statement of originality

Here, we highlight the original parts in this study. In Chapter 2 we obtain new solutions of battery model in dilute electrolyte theory. In Chapter 3, we review the existing moderately concentrated electrolyte model (originally formulated in [59]) and highlights some errors and give corrections. In Chapter 4, we extend the results of the homogenisation in [74] to a battery model in moderately concentrated electrolyte. The numerical procedure developed in Chapter 6 to solve battery problems is new and is very efficient. The results in Chapter 7 follow the work of Srinivasan and Newman [85] for a half

cell anode but are significantly extended and provide considerably better agreement to experimental data. The results for the half cell cathode in Chapter 8 are all new.

Chapter 2

Dilute electrolyte modelling of battery

2.1 Introduction

In this section we develop a battery model based on dilute electrolyte theory. We start in §2.2, by discussing a model for a dilute electrolyte. We then discuss lithium transport between the electrolyte and the electrode particles in §2.3 before briefly discussing transport in the electrode particles in §2.4 and illustrating how homogenisation can be used to derive a model on the scale of the battery model in §2.5. In §2.6 and §2.7 we derive some solutions to this battery scale model that illustrate the behaviour of a certain class of cell.

2.2 Derivation of a model for a dilute electrolyte

The Nernst-Planck theory has been used to describe a sufficiently dilute electrolyte [60]. This theory describes conservation equations for the ionic species that diffuse by ionic concentration gradient and advect by an electric field. Here we discuss the derivation of battery model in a dilute electrolyte, which previously has been described in Richardson *et al.* [74].

The general conservation of mass equation for two species, concentrations c_n^* and c_p^* (mol m^{-3}), that diffuse independently are

$$\frac{\partial c_i^*}{\partial t^*} + \nabla \cdot \mathbf{q}_i^* = 0 \quad \mathbf{q}_i^* = -D_i \nabla c_i^* \quad \text{for } i = n, p. \quad (2.1)$$

where \mathbf{q}_i^* is the ion flux of species i . The second equation is Fick's Law of diffusion which states that the diffusive flux is proportional to the concentration gradient. Here D_n and